ANALYSIS OF COMPLEX PASSIVE (M)MIC-COMPONENTS USING THE FINITE DIFFERENCE TIME-DOMAIN APPROACH

M.Rittweger and Ingo Wolff, Fellow, IEEE

Department of Electrical Engineering and Sonderforschungsbereich 254
Duisburg University, Bismarckstr. 69, D-4100 Duisburg, FRG

ABSTRACT

The analysis of a number of complicated microstrip components containing coupled discontinuities and line structures using the finite difference time-domain (FDTD) method is presented. The time-domain data are plotted and the frequency-domain response in form of S-parameters is compared with accurate measurements. Advantages and disadvantages of the applied technique are discussed and modifications of the available algorithms for increased efficiency and stability of the solutions are described.

INTRODUCTION

First applications of the three-dimensional finite difference time-domain method (FDTD-method) to planar microwave circuits have been reported by [1,2]. The FDTD-method is a numerical method for the solution of electromagnetic field problems which has a large numerical but a low analytical expense. Despite this large numerical expense it is believed to be one of the most efficient techniques, because basically it only stores the field distribution at one time moment in memory, instead of working with a large system matrix relating several unknowns. The field solution for each other time is determined by Maxwell's equations and is calculated here using a time-stepping procedure based on the finite difference method. The used leapfrog algorithm fits very well on modern computer architectures, so that the data required to describe a three-dimensional field distribution can be handled in a reasonable time.

The transient analysis delivers the broadband frequency response in one single computation run. A simulation of absorbing boundaries is necessary to match the ports using a finite discretized space and therefore a finite computer memory.

BOUNDARY TREATMENT

In [1] a very simple and therefore efficient algorithm for the simulation of absorbing boundaries based on the super-absorption method is used. With the assumption of a wave incident normally to the boundary and a phase-velocity v_{ph}, which is not frequency dependent, the relation of the spatial shape and the time behaviour of a pulse, or a wave as a spectral component of it, is used to determine the field on the boundary. This means, that the field one space-step displaced from the absorbing boundary after a time delay

$$t_O = \frac{\Delta h}{v_{ph}} \tag{1}$$

where t_O is the time the pulse needs to travel one space-step Δh on the transmission line, fixes the field on the boundary. Due to the violation of the assumptions mentioned above for pulse propagation in real microwave components, the same procedure is made a half step displaced from the absorbing boundary and an error cancellation algorithm improves the absorption. It can be shown, that the described boundary algorithm, which fulfills the wave equation exactly in the case of a non-dispersive and single direction wave propagation, also allows wave excitation in the opposite direction in the air-filled area for a frequency f_{osc} corresponding to the period

$$T_{osc} = t_O + \frac{\Delta h}{c} \quad , \tag{2}$$

which is t_O plus the time a wave needs to travel one space-step in air. So stability of the absorbing boundary is not given for f_{osc}. Alternative absorbing boundary conditions without this disadvantage are normally of less order or to expensive. But due to the fact, that the absorbing boundary algorithm described above offers a number of field-samples over the actual moment in time, together with buffered samples of passed moments, digital filter techniques even with non causal systems can be used to suppress oscillation of the absorbing boundary. The simplest method is building an average of some neighboured samples means

CH2848-0/90/0000-1147$01.00 © 1990 IEEE

nothing else but the convolution with a rectangular function with a width T_{osc} or multiplying the boundary field with a real lowpass filter function

$$H(f) = \frac{f_{osc}}{\pi f} \sin\left(\frac{\pi f}{f_{osc}}\right) \qquad (3)$$

in the frequency-domain. This will not touch the frequencies incorporated in the stimulated pulse very much, but improves stability of the absorbing boundaries, so that it is no longer necessary to choose such a large computation domain as before.

MATCHED SOURCES

In [1] the problem of matched sources was solved by separating the stimulated pulse and the reflected part of it by using a transmission line connected to the component under test, which is long compared to the pulse width. After the pulse has left the excitation plane the reflected pulse propagates through an absorbing boundary which is switched on at this time. There has to be a distance between the excitation plane and this absorbing boundary, because the homogenous pulse excitation induces a dc-offset in the tangential H-field due to the violation of Maxwell's equations. Accuracy recommends the use of an excitation pulse, whose duration is sufficiently long. Arbitrarily long pulse durations can be used if matched sources are available. They can be simulated by separating the calculation domain in two parts. The first part contains only a transmission line which can be excited in the conventional way. The transmission line is terminated with an absorbing boundary at the other end and it should be long enough to stabilyze the pulse form after excitation and furthermore to let the mentioned dc-offset of the H-field vanish. The field close to the termination of this line, which is a real physical solution, is used to excite the second part of the computation domain containing the component connected to short transmission lines. In this area superposition of pulse propagation in both directions is allowed. The absorbing boundary algorithm can be used for the reflected part as before, because separation of the transmitted and reflected part of the pulse is possible using the information of the first computation domain. A symmetry of the transmission line in the first computation domain can be used even if there is no symmetry in the component to be analyzed.

EXAMPLES

The FDTD-method offers the possibility of a flexible problem formulation with an analytical expense which is much lower than e.g. that of spectral domain analysis techniques. Arbitrarily shaped planar line discontinuities, as e.g. the circular shape of a radial stub (Fig. 1), can easily be approximated in a rectangular mesh. Even very rough mesh sizes lead to acceptable accuracy of the results. As an example for this thesis the circular radial stub [5] connected to two closely coupled microstrip bends (Fig. 1) has been discretized with only three spatial steps over the width of the microstrip line and the substrate height. Nevertheless, as a comparison of the calculated S-parameters (Fig. 1) with accurate measurements [4] (using the time-domain option of a network analyzer) shows, the amplitude and phase response of this complicated structure is described very accurately, only at higher frequencies a small frequency offset can be found because of the large mesh size which is not able to resolve spectral components of higher frequencies i.e. short wavelengths. It is interesting to mention that the discretization error does not result in an amplitude error but only in a frequency offset. In Fig. 2 additional information of the electromagnetic field inside the structure is given by the time dependent E_Z field component over the substrate area.

It could be found that the accuracy of the solution at higher frequencies can be improved by assuming only one more grid point over the width of the microstrip line.

The FDTD-method is a real three-dimensional analysis technique which for the first time allows to analyze complicated three-dimensional microwave components with an acceptable computational expense. The calculated and measured results for a planar microwave rectangular inductor (Figs. 3 and 4), considering all coupling effects of the lines and between the discontinuities as well as the transmission properties of an air-bridge from the inside of the coil accurately, show that the agreement between analysis and measurements is very good even at higher frequencies. It should be recognized that even the phase response which has been a critical aspect in nearly all other calculation methods is predicted with a high accuracy by the FDTD-method.

The authors selected the distributed inductor as an example because all resonant phenomenas were intended to be in a frequency area, that allows to verify the simulation by measurements. Smaller dimensions lead to higher resonant frequencies but don't take influence on the simulation. A problem is, that the calculation cannot describe physical reality, if the assumptions made in the use of Maxwell's equations are not valid, i.e. if e.g. the material properties or probably any losses are dominantly frequency dependent. However, the analyzed examples make believe that at least in their case errors caused from the discretized nature of the FDTD-method are important.

ERRORS

The essential errors occuring are very similar to that of the related transmission line matrix (TLM) method [6]. First this is the so called coarseness error i.e. the discretization in space is not able to resolve high non-uniform fields for example at the edge of a metallization. In [3] a method for incorporation of edge singularities is introduced showing that the geometrical dimensions of the metallization are assumed too small, if the contour is placed exactly on the field nodes as it was taken in the considered examples. Another error, which also can be corrected, is the velocity error which describes the numerical dispersion of the leapfrog method. This error causes a frequency shift of less then 0.3 percent for the given examples. Reflections at the absorbing boundaries as well as the assumption of single mode propagation for the S-parameter determination cause errors too. Furthermore the truncation of the infinite pulses in time-domain may result in ripples in the frequency response.

CONCLUSION

Complicated microstrip components including real three-dimensional structures were analyzed using the FDTD-method to simulate pulse propagation in the time-domain considering radiation effects. S-parameters received via Fourier transforms show good agreement with the compared measurements. Errors and error correction techniques have been discussed.

References

[1] X. Zhang, and K. K. Mei, "Time-domain finite difference approach to the calculation of the frequency-dependent characteristics of microstrip discontinuities," *IEEE Trans. Microwave Theory and Tech.*, vol MTT-36, pp. 1775-1787, Dec. 1988.

[2] X. Zhang, J. Fang, and K. K. Mei, "Calculations of the dispersive characteristics of microstrips by the time-domain finite difference method," *IEEE Trans. Microwave Theory and Tech.*, vol. MTT-36, pp. 263-267, Feb. 1988.

[3] C. J. Railton, and J. P. McGeehan, "Analysis of microstrip discontinuities using the finite difference time domain technique," IEEE MTT-S Digest, pp. 1009-1012, June 1989.

[4] G. Gronau, and I. Wolff, "A simple broad-band device de-embedding method using an automatic network analyzer with time-domain option," *IEEE Trans. Microwave Theory and Tech.*, vol. MTT-37, pp. 479-483, Jan. 1989.

[5] W. Wertgen, "Elektrodynamische Analyse geometrisch komplexer (M)MIC- Strukturen mit effizienten numerischen Strategien," Ph.D. Thesis, Duisburg University, FRG, 1989.

[6] W. J. R. Hoefer, "The transmission-line matrix method - theory and application," *IEEE Trans. Microwave Theory and Tech.*, vol. MTT-33, pp. 882-893, Oct. 1985.

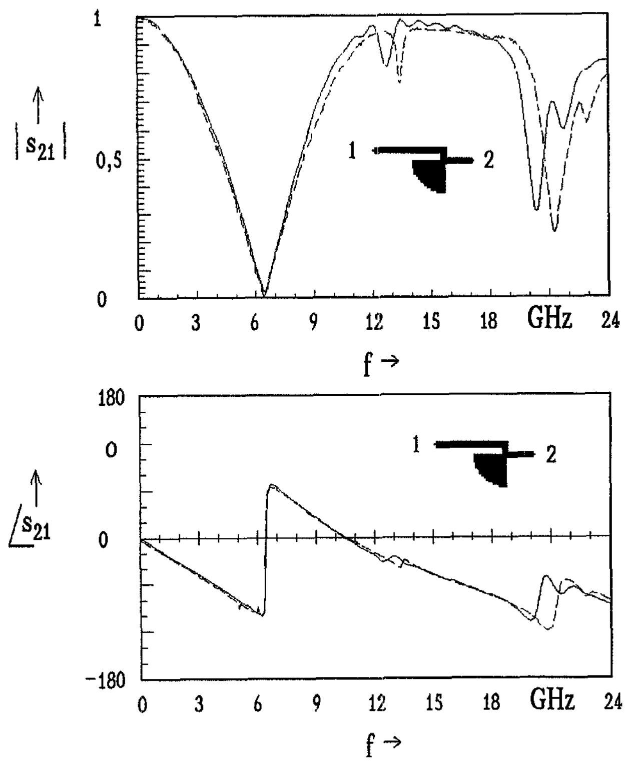

Fig. 1: Calculated (——) and measured (– – –) S-parameters of the radial stub. Al_2O_3, ε_r = 9.768 (measured), height = .635 mm, width = .61 mm, gap = .61 mm, radius = 3.253 mm.

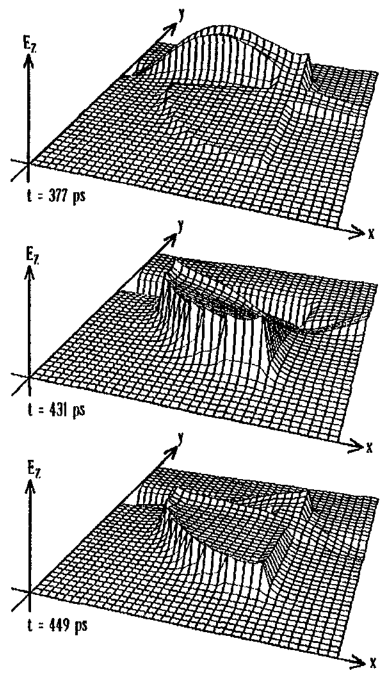

Fig. 2: Time-dependent E-field perpendicular to the substrate under the metallization of the radial stub.

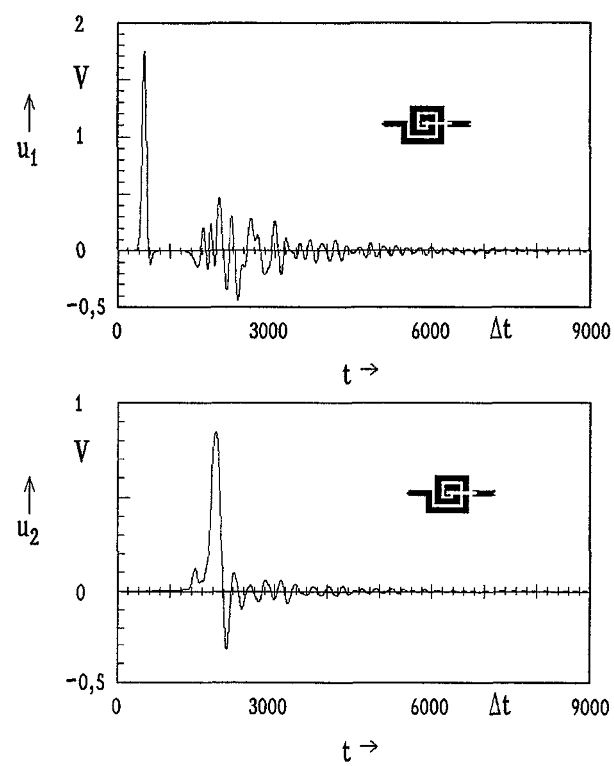

Fig. 3: Voltage history at port 1 (left port) and port 2 (right port) of the spiral inductor. Al_2O_3, $\varepsilon_r = 9.8$, height = .635 mm, width = .625 mm, gap = .3125 mm, air-bridge diameter = .3125 mm.

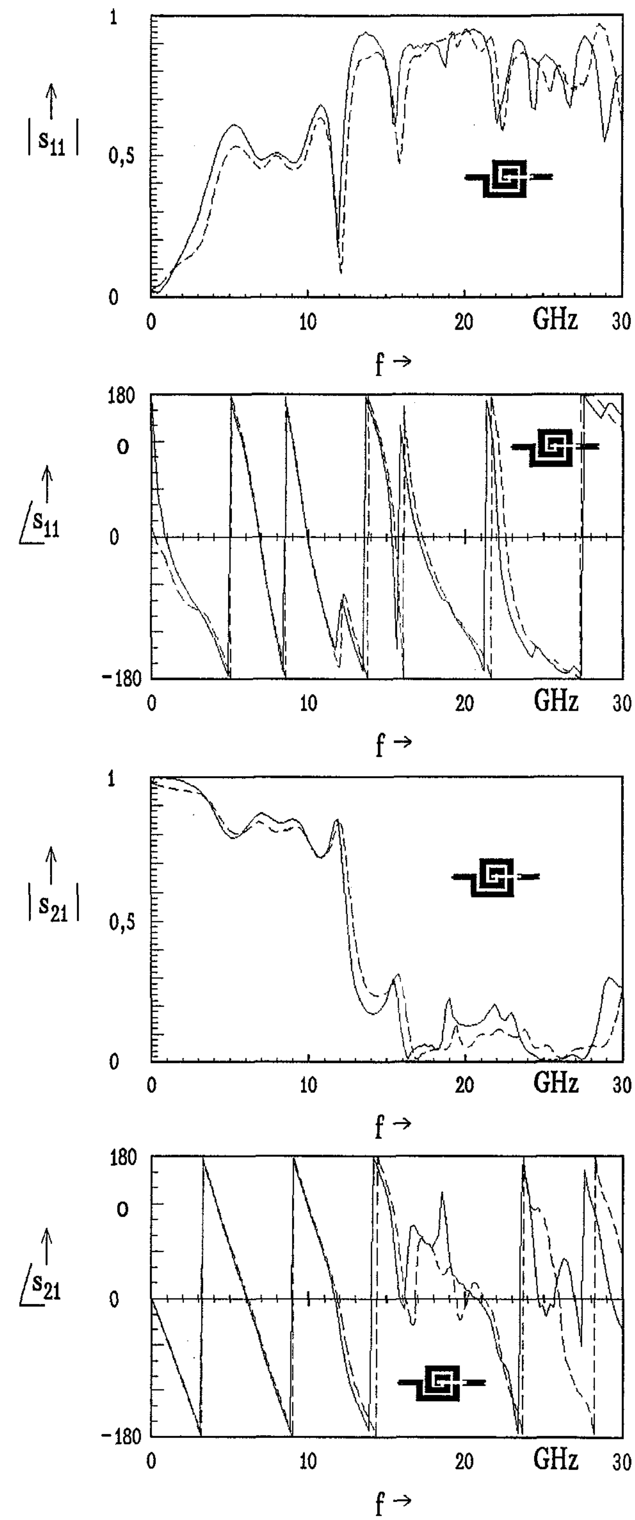

Fig. 4: Calculated (——) and measured (– – –) S-parameters of the spiral inductor.